Permanent Dipole of Metal−Benzene Molecules: Evidence for Long-Range Weakly Bound States?

F. Rabilloud, D. Rayane, A. R. Allouche, R. Antoine, M. Aubert-Frécon, M. Broyer, I. Compagnon, and Ph. Dugourd*

Laboratoire de Spectrométrie Ionique et Moléculaire, UMR 5579 (Université Lyon1 & CNRS) 43 Bd du 11 Novembre, 69622 Villeurbanne Cedex, France

Received: May 21, 2003; In Final Form: October 7, 2003

Electric deflection experiments have been performed on metal−benzene compounds (for scandium, vanadium, nickel, niobium, and tantalum). CASSCF + MRCI calculations are reported for Sc, V, and Ni complexes. The lowest energy structures correspond to long-range states (distance between the metal atom and the center of the benzene molecule superior to 4 Å), while the short-range states are metastable against dissociation. The comparison between experimental results and theory demonstrates the importance of these long-range states.

1. Introduction

Research on metal−ligand molecules in the gas phase has exploded these past years with the development of laser vaporization sources. Transition-metal−benzene complexes are of particular broad interest. On the fundamental point of view, the study of transition-metal−benzene complexes can provide a basic model for understanding d−π binding interactions[1] and be used to build new cluster assembled materials. For example, organometallic polymers made of an alternation of metal atoms and benzene rings could provide a new class of one-dimensional conductors.[2]

In recent works, Kaya and co-workers have successfully synthesized neutral 3d transition-metal−benzene complexes $M_n(C_6H_6)_m$ by using molecular beam methods.[3,4] From magic numbers in mass spectra, chemical reactivity, and theoretical inputs, they showed that two different families of structures are observed. Scandium, titanium, and vanadium complexes have a multiple-decker sandwich structure (n, $m = n + 1$ compounds), in which metal atoms and benzene molecules are alternatively stacked in a one-dimensional structure. On the other hand, for Fe, Co, and Ni, a rice-ball structure is observed. In that structure a metal cluster is covered by benzene molecules. Ion mobility experiments on $V_n(C_6H_6)^+_n$ complexes[5] and IR spectroscopy on $V(C_6H_6)^+_{1,2}$ complexes[6] have confirmed the stability of the sandwich structures. Armentrout and co-workers have performed collision-induced dissociation (CID) experiments and have obtained thermochemistry data on metal−ligand $M(C_6H_6)^+_{1,2}$ complexes.[7] Recently, Kasai and co-workers, using the method of electrostatic hexapole field,[8] have reported electric dipole measurements on $Ti(C_6H_6)$ and $Ti(C_6H_6)_2$ molecules.[9] For the $Ti(C_6H_6)$ molecule, they obtained 2.4 ± 0.3 D. We have also reported electric dipole measurements for a series of transition-metal−$(C_6H_6)_2$ sandwiches.[10]

While sandwich structures are well characterized, few results exist on the MC_6H_6 molecules. Despite a wide theoretical effort,[11−15] the fundamental electronic state of these molecules is not fully characterized yet. The main difficulty to describe these systems comes from the existence of open d electronic shells and of numerous low-energy electronic states. In particular, the spin multiplicity of the ground state is difficult to determine, and different theoretical approaches may lead to controversial results. Experimental results are available for complexes in a matrix. Electron paramagnetic resonance (EPR) and electron spin resonance (ESR) measurements have shown that metal−benzene complexes in matrixes have low-spin ground states.[16−18] There are no definitive experimental results in the gas phase. Magnetic dipole measurements would allow a direct experimental probe of the spin multiplicity, but have not been performed yet. Electric dipole measurements that probe the charge distribution of the molecule ground state may be an alternative approach to characterize these molecules. In this paper, we present the measurement of the electric dipole moment of isolated MC_6H_6 molecules for some first-, second-, and third-row transition-metal atoms. For first-row transition-metal atoms (M = Sc, V, Ni), experimental results are compared to CASSCF + MRCI calculations.

2. Experiment

Electric dipoles of free neutral complexes are measured by deflecting a molecular beam in an inhomogeneous electric field.[19] The experiment consists of a laser vaporization source coupled to an electric deflector and a mass spectrometer. Metal atoms (M) are vaporized from a 6 mm metal rod using the frequency-doubled output of a Nd^{3+}:YAG laser (532 nm). Metal atoms are carried out by a pulse of helium gas synchronized on the vaporization laser pulse. The helium carrier gas contains a small amount of benzene introduced with a temperature-controlled container connected by a tee to the helium line (the partial vapor of benzene is ≤0.1 bar). Metal atoms react with benzene molecules in the main chamber and in the nozzle to form metal−benzene complexes. The molecules are thermalized to room temperature in the 5 cm long nozzle.

After two skimmers, the beam is collimated by two 0.5 mm slits and goes through a 15 cm long electric deflector. The geometry of the deflector provides both an electric field F (F = 0 to 1.63×10^7 Vm^{-1}) and a field gradient $\partial F/\partial Z$ (0 to 2.82×10^9 Vm^{-2}). The direction Z of the field and of its gradient is

* To whom correspondence should be addressed. E-mail: dugourd@lasim.univ-lyon1.fr.

10.1021/jp035403a CCC: $25.00
Published on Web 12/02/2003

perpendicular to the beam axis. The molecules are ionized 1 m after the deflector in the extraction region of a position-sensitive time-of-flight mass spectrometer. A low-fluence ArF laser is used for the ionization ($\lambda = 193$ nm, and $E = 1$ mJ/cm^2 per pulse). The arrival time at the detector is a function of the mass of the particle and of the deviation d of the beam.

The deviation d of a molecule is given by

$$d = K\langle f\rangle/mv^2 \quad (1)$$

where $\langle f\rangle$ is the average force in the deflector on the molecule, v and m are the velocity and the mass of the molecule, and K is a geometrical factor that was calibrated on the sodium atom whose polarizability is known with a high accuracy from atomic interferometry.[20] The velocity is selected and measured with a mechanical chopper. The velocity was typically 1430 ± 43 ms^{-1}. The average force on a rigid polar molecule is

$$\langle f\rangle = \mu\langle\cos\theta\rangle\nabla F + \alpha_e F\nabla F \quad (2)$$

μ is the permanent dipole of the molecule, θ is the angle between the permanent dipole and the electric field direction, and α_e is the electronic polarizability of the molecule. $\langle\cos\theta\rangle$ is the average value of cos θ calculated in the electric field. The force due to the electronic polarizability is small as compared to the force due to the permanent dipole, and the second term in the right-hand part of eq 2 can be neglected.

3. Experimental Results

Metal−benzene molecules with M = Sc, V, Ni, Nb, and Ta atoms were studied in this work. The mass spectra of $M_n(C_6H_6)_m$ clusters that we obtained are similar to those published by Kaya and co-workers.[3,4] Due to the high chemical reactivity of transition-metal atoms with benzene molecules, the most intense species observed in the mass spectra contain more than one molecule of benzene when the partial vapor pressure of benzene in helium is about 0.1 bar. To efficiently produce MC_6H_6 molecules, it is necessary to reduce the benzene concentration in the carrier gas to less than 10^{-3} bar.

Typical arrival time distribution profiles of MC_6H_6 measured with and without an electric field in the deflector (0 and 15 kV) are shown in Figure 1 for Sc, V, and Ni metal atoms. For ScC_6H_6 (Figure 1a), the first peak in the time-of-flight mass spectrum corresponds to a molecule of the residual vacuum (mass 122 amu). The second peak corresponds to ScC_6H_6. The profile of this second peak is strongly broadened when the field is turned on in the deflector. This broadening in arrival time at the detector is due to a spreading of the molecular beam induced by the electric field in the deflector (eq 2).[19] For vanadium (Figure 1b), the effect of the electric field is weak. The double peak observed in the arrival time distribution spectrum for the NiC_6H_6 molecule is due to the isotopic distribution of the nickel atom ($^{58}NiC_6H_6$ mass 136 amu and $^{60}NiC_6H_6$ mass 138 amu). A significant broadening of the peaks is observed when there is an electric field in the deflector.

Profiles of deviation were systematically recorded as a function of the voltage across the deflector. Results are reported in the right part of Figure 1. A regular decrease in the signal is observed as the voltage increases, it is a measure of the broadening of the beam. The error bars correspond to the statistical dispersion of the values deduced from various experiments. The precision in the relative intensity depends on the stability of the signal and on the signal-to-noise ratio. It is necessary to add to this uncertainty the ones resulting from the velocity measurement and from the calibration.

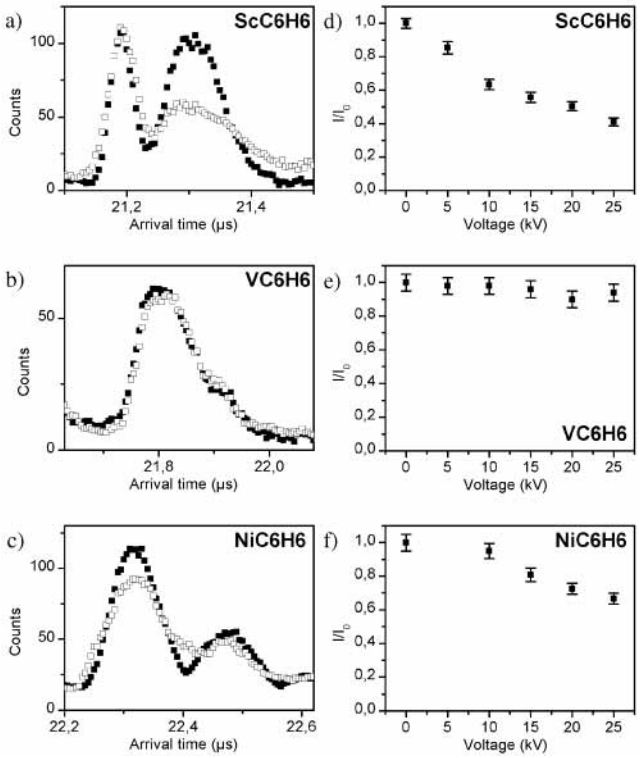

Figure 1. (a−c) Arrival time distribution profiles measured for MC_6H_6 molecules, M = Sc, V, Ni: ■, profile without an electric field in the deflector (0 kV); □, profile with a voltage of 15 kV across the deflector ($F = 8.8 \times 10^7$ V/m). (d−f) Relative intensity at the maximum of the MC_6H_6 peak as a function of the voltage across the deflector. The decrease in intensity is a measurement of the broadening of the beam profile due to the electric field in the deflector.

4. Quantum Chemical Calculations

a. Method. We have performed ab initio calculations to investigate the potential energy profile of the electronic ground state and some lower lying excited states having various spin values or spatial symmetries. One of our goals was to determine the spin multiplicity of the ground state. Due to the open d-shell structure, transition-metal systems have several spin-multiplet symmetries lying within a narrow energy range. For such systems, the use of single-reference-based approaches, such as CCSD(T) or DFT, will tend to favor states with the highest spin multiplicities. Multireference techniques where electronic wave functions are treated as multiconfigurational functions are more suitable for the characterization of the multiplicity of the ground state. In such a sense, we have performed CASSCF (complete active space self-consistent field) + MRCI (multireference configuration interaction) type calculations by use of the computational chemistry program MOLPRO.[21] As is well-known, those calculations are computer intensive, and consequently, they were done only for MC_6H_6 with M = Sc, Ni, and V.

Metal atoms were represented through the relativistic effective core pseudopotential developed by Dolg et al.[22] replacing 10 core electrons. For carbon, the $1s^2$ core was replaced by a similar pseudopotential.[23] We occasionally used pseudopotentials developed by Stevens et al.,[24,25] but as the results were found to be very similar, we will only discuss the calculations performed with the pseudopotential of Dolg et al. The Gaussian basis sets for metal atoms were (8s7p6d1f) contracted in [6s5p3d1f] from

ref 22, that for carbon was [4s2p], and that for hydrogen was a DZP basis as displayed in MOLPRO.

The potential energy profiles were calculated at the CASSCF level. The active space included the metal 4s, 3d, 5s, and 4d orbitals. The inner orbitals of the metal and orbitals of the benzene molecule were kept inactive in the CAS process but were allowed to relax in the SCF process. For the geometry optimization we changed only the distance between the metal atom and the center of mass in the benzene molecule. Namely, the benzene molecule structure was not allowed to relax and was fixed to the isolated one optimized from a CASSCF calculation. Then a single-point MRCI (single and double excitations) type of calculation was performed at the CASSCF equilibrium geometry for the lower energy states for each spin multiplicity to determine the dipole moment. For these calculations, the basis set was further augmented by diffuse functions on both the metal atom and benzene molecule, though they seemed to yield a very small improvement.

Calculations were performed in the C_{2v} point group, but the C_{6v} symmetry of the MC_6H_6 complex was maintained throughout. However, we occasionally performed a local optimization (in the C_{2v} point group) to investigate the rigidity of the benzene molecule. This was the case for NiBz, for which the distance between the metal atom and benzene molecule was found to be shorter than it was for the other complexes, so the possible distortion was expected to be bigger. We found only a small distortion: the C−C and C−H distances were found to be 1.405 and 1.068 Å, respectively, to be compared with the values of 1.386 and 1.071 Å, respectively, for isolated benzene. The C_{6v} symmetry of the complex was not broken, but hydrogen atoms were found to move from their initial position to a plane parallel to the carbon ring and located 0.021 Å below it, and then more distant from the atom metal located above the carbon ring. Nevertheless, the deformation was not significant for the present study, and the C_{6v} symmetry constraint with a rigid ring for benzene appeared to be appropriated. The possibility of the existence of the asymmetric-top molecules was also investigated for both NiC_6H_6 and ScC_6H_6 complexes. Local optimizations with the metal atom placed above the benzene plane but displaced from the center axis (C_s symmetry) were found to converge either in a perfectly symmetric structure or in dissociation into C_6H_6 + metal atom.

b. Results. Before the results of the calculations are shown, it is useful to review the bonding scheme in transition-metal−benzene systems. The valence configuration of the isolated transition-metal atoms which are considered in the present study is $3d^n4s^2$ with the 3d orbitals split into $3da_1$ (d_{z^2}), $3de_1$ (d_{xz} and d_{yz}), and $3de_2$ ($d_{x^2-y^2}$ and d_{xy}) in C_{6v} symmetry. For the lower lying states of the MC_6H_6 complex, the ligand orbitals will not be placed between the metal orbitals, and the order of the valence orbitals will be a_1, e_1, and e_2 (from the σ and π occupied orbitals of benzene) and 4s/3d (partially filled from the transition-metal atom). As the 4s orbital has a repulsive interaction with the doubly occupied benzene a_1 orbitals, the molecular diabatic state built from the $3d^n4s^2$ ground-state atomic configuration is repulsive. On the contrary, an excited atomic state having a $3d^{n+2}$ configuration has an attractive interaction with the benzene molecule, resulting in a stabilization of energy in a diabatic curve. Thus, these two diabatic potential energy curves intersect each other, resulting in a ground-state adiabatic potential energy curve which presents a barrier of dissociation derived from the avoided crossing. For the ground state, the electronic configuration at the minimum energy will be primarily $3d^{n+2}$ or $3d^{n+1}4s^1$, while that at the dissociation limit will be $3d^n4s^2$.

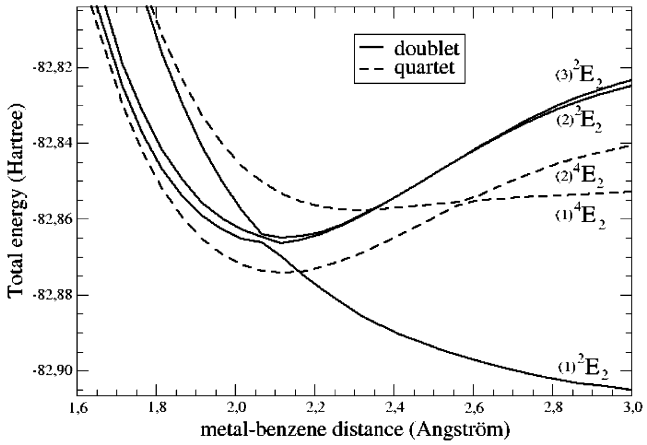

Figure 2. Short-range calculated potential energy curves for the ScC_6H_6 molecule: solid lines, doublet states; dashed lines, quartet states.

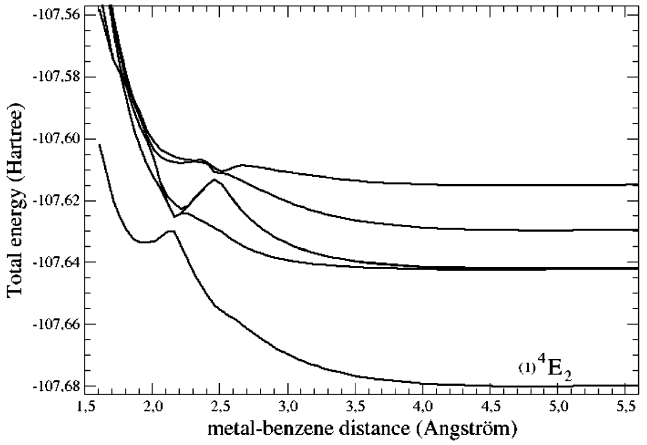

Figure 3. Potential energy curves for the $^4E_2$ states for the VC_6H_6 molecule.

This bonding scheme is illustrated for ScC_6H_6 in Figure 2, where the potential energy curves of the lower lying doublet (solid lines) and quartet (dashed lines) are shown. For doublet states, avoided crossings involving several diabatic states with a primarily $4s^23d^1$ or $4s^13d^2$ electronic configuration occur within the 2.05−2.15 Å range of the Sc−C_6H_6 distance. They result either in metastable states with respect to the dissociation in C_6H_6 + Sc and having a $4s^23d^1$ asymptote or in stable states with respect to the $4s^13d^2$ asymptote. For quartet states, the avoided crossing between the two lower lying states, which have $4s^13de_2^2$ and $4s^13de_23da_1$ electronic configurations, results in two stable states with respect to the $4s^13d^2$ asymptotes. The lowest energy state (at short distance) for ScC_6H_6 is found to be a quartet ((1) $^4E_2$ state) lying 0.21 eV below the doublet state ((2) $^2E_2$ state). The dissociation energy to the $4s^13d^2$ asymptote is found to be 0.80 eV in good agreement with the CCSD(T) value of 1.03 eV by Hong et al.[26] Close to the dissociation limit (20 Å), the lowest state is calculated to be a doublet located 1.79 eV below the quartet. This value overestimates the experimental atomic excitation energy (1.43 eV) from the doublet (^2D) to the quartet (^4F) by about 0.36 eV.[27]

The ground state for VC_6H_6 is found to have a quartet multiplicity and to be metastable with respect to the dissociation in C_6H_6 + V with an energy barrier of 0.11 eV (see Figure 3). A doublet state is found lying 0.44 eV above the quartet, while the sextet is found to be completely repulsive. These results

TABLE 1: Calculated Relative Energy (eV), Metal−Ring Distances *d* (Å), and Dipole Moments μ (D) for MC_6H_6[a]

					Mulliken population on the metal atom			
metal	state	energy	d	μ	s	p	d	net charge on the metal atom
Sc	(1) $^2E_2$	0.00	4.96	0.90	1.84	0.17	1.01	−0.02
	(1) $^4E_2$	1.05	2.12	2.27	0.96	0.60	1.57[b]	−0.19
	(2) $^2E_2$	1.26	2.12	3.15				
	(3) $^2E_2$	1.30	2.12	2.44				
V	(1) $^4E_2$[c]	0.00	4.82	0.60	1.92	0.07	3.03	−0.02
	(1) $^6A_1$	0.60	4.30	1.17	1.00	0.02	4.01	−0.03
	(1) $^4E_2$[d]	1.26	1.97	2.79	0.96	0.59	3.55	−0.10
	(1) $^2E_2$	1.70	1.91	3.70	0.96	0.64	3.53	−0.13
	(2) $^2E_2$	2.08	4.92	0.67				
Ni	(1) $^3E_2$	0.00	4.62	0.47	2.00	0.01	8.00	−0.01
	(1) $^1A_1$	0.48	4.17	0.90	1.00	0.02	9.00	−0.02
	(2) $^1A_1$	0.78	1.62	0.49	0.33	0.54	9.35	−0.22

[a] The dipole moment is oriented from M to Bz. The net charge and the Mulliken population on the metal atom are also given. [b] For the ScC_6H_6 (1) $^4E_2$ state, there is 0.06 electron on the f orbitals. [c] Long-range minimum. [d] Short-range minimum.

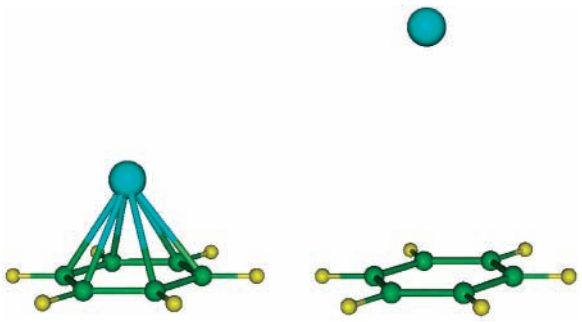

Figure 4. Geometry of the VC_6H_6 molecule at the short-range (left) and long-range (right) minima of the lowest energy state ((1) $^4E_2$ state).

are in very good agreement with those of the ab initio study by Yasuike et al.[28] using a full valence configurational interaction method with configuration-averaged SCF orbitals. However, Pandey et al. with DFT/BPW91 calculations[11] have obtained a spin multiplicity of 6 for the ground state with a $4s^13de_2^23de_1^2$ electronic configuration, while this state is found to be not stable at short range in the present study. Although DFT calculations are known to favor the highest spin multiplicity, it is difficult to conclude definitively on the spin multiplicity of VC_6H_6 since there have been no experimental reports in the gas phase.

The lowest energy short-range state for NiC_6H_6 is found to be a singlet and to be metastable with respect to the dissociation in C_6H_6 + Ni with an energy barrier of 0.14 eV. The lowest triplet states were found to be repulsive, and the first short-range-lying triplet state was found to be bound at about 1.7 eV above the doublet one.

Up to now we have only discussed the short-range-bound states, say with a metal−benzene distance below 2.5 Å. In fact, some molecular states were found to be slightly bound at long range, within 4−5 Å for the metal−benzene distance. The most stable short- and long-range geometries for VC_6H_6 are shown in Figure 4. For the three complexes considered here the long-range binding energies are found to be about 300 K at the MRCI plus Davidson correction level of calculation. For ScC_6H_6, a doublet bound state was found with a metal atom−benzene distance of 4.96 Å and a dissociation energy of 260 K. For VC_6H_6, the quartet state was found to be bound with a V−benzene distance of 4.82 Å and with a binding energy of 350 K. This state lies 0.60 eV below the sextet, which is bound at long range with a binding energy of 520 K. For NiC_6H_6, a singlet state and a triplet state were found to be stable with a binding energy of about 360 K. We emphasize that these values are only estimations of the binding energy and that they may underestimate the real values.

For both short-range- and long-range-bound states, calculated energy and dipole results are given in Table 1. The net charge and the s, p, and d orbital populations on the metal atom obtained through a Mulliken analysis are also given in this table. The long-range-bound states have weak dipoles, due to a residual charge transfer. Spin multiplicity changes between the atom and the complex are related to the promotion of an electron from an s orbital to a d orbital due to the influence of the benzene molecule.

5. Discussion

The present calculations outline that the minima of the short-distance states are above the dissociation energy of the molecule, which corresponds to the energy of the benzene molecule and of the metal atom in their ground states. These states are metastable with respect to benzene and metal atom ground states. Only long-range states are stable against dissociation. In the following, we discuss the possible observation of long-range states by comparing the results of deflection experiments to calculations.

This comparison is done by plotting the intensity at the maximum of the peak as a function of the electric field in the deflector for every calculated state. We have simulated the effect of the electric field for each calculated state with a classical approach.[19] In a static field the Lagrangian of a symmetric-top molecule is

$$L = \frac{I_1}{2}(\dot{\theta}^2 + \dot{\varphi}^2 \sin^2\theta) + \frac{I_3}{2}(\dot{\psi} + \dot{\varphi}\cos\theta)^2 + \mu_0 F \cos\theta \quad (3)$$

where θ, φ, and ψ are the Euler angles, θ giving the inclination of the axis of the symmetric-top cluster from the direction Z of the electric field. p_θ, p_φ, and p_ψ are the conjugate momenta. I_1 is the value of the two equal momenta of inertia of the complex, and I_3 is the value of the third momentum of inertia (the values of the rotational constants for the calculated structures are given in Table 2). Using eq 3 and adiabatic invariants (p_φ, p_ψ, and $\oint p_\theta \, d\theta$),[19] the average value of cos θ can be calculated as a function of p_φ, p_ψ, and the initial energy E_0 of the molecule. The average force is deduced from $\langle\cos\theta\rangle$ using eq 2. To obtain a profile, every initial configuration is taken into account with a Boltzmann weight. There is no supersonic expansion at the exit of the nozzle, and the rotational temperature used in the calculation is the temperature of the nozzle (300 K). Here, this temperature has very little influence on the calculated profiles,

TABLE 2: Calculated Rotational Constants (cm^{-1}) for the Calculated States of MC_6H_6 (See the Text)

metal	state	A (cm^{-1})	C (cm^{-1})
Sc	(1) $^2E_2$	0.0206	0.0963
	(1) $^4E_2$	0.0783	0.0963
	(2) $^2E_2$	0.0783	0.0963
	(3) $^2E_2$	0.0783	0.0963
V	(1) $^4E_2$[a]	0.0210	0.0963
	(1) $^6A_1$	0.0257	0.0963
	(1) $^4E_2$[b]	0.0816	0.0963
	(1) $^2E_2$	0.0833	0.0963
Ni	(1) $^3E_2$	0.0210	0.0963
	(1) $^1A_1$	0.0251	0.0963
	(2) $^1A_1$	0.0951	0.0963

[a] Long-range minimum. [b] Short-range minimum.

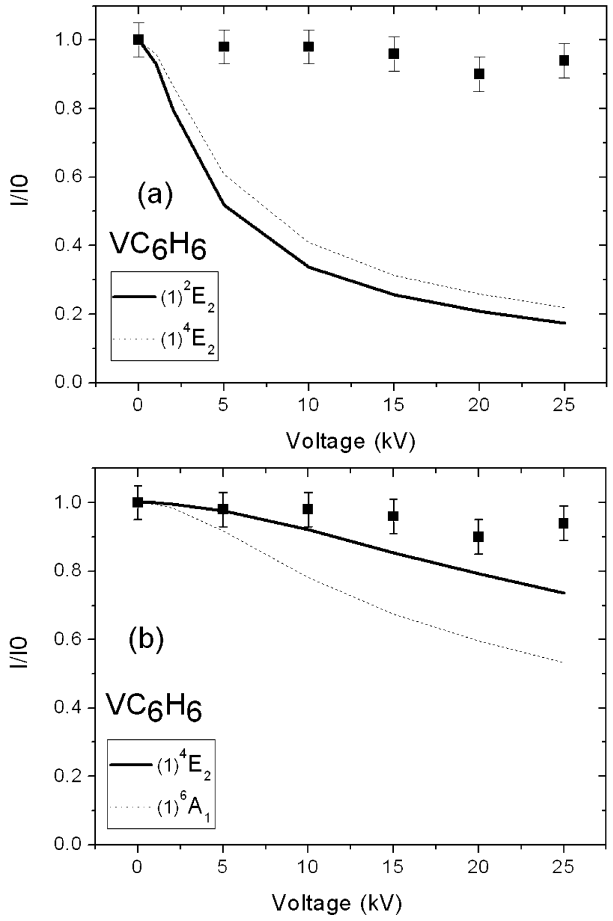

Figure 5. Relative intensity at the maximum of the VC_6H_6 peak as a function of the voltage across the deflector. (a) Experimental results (■) and simulations for short-range states: (1) $^4E_2$ state ($\mu = 2.79$ D) and (1) $^2E_2$ state ($\mu = 3.7$ D). (b) Experimental results (■) and simulations for long-range states: (1) $^4E_2$ state ($\mu = 0.6$ D) and (1) $^6A_1$ state ($\mu = 1.17$ D).

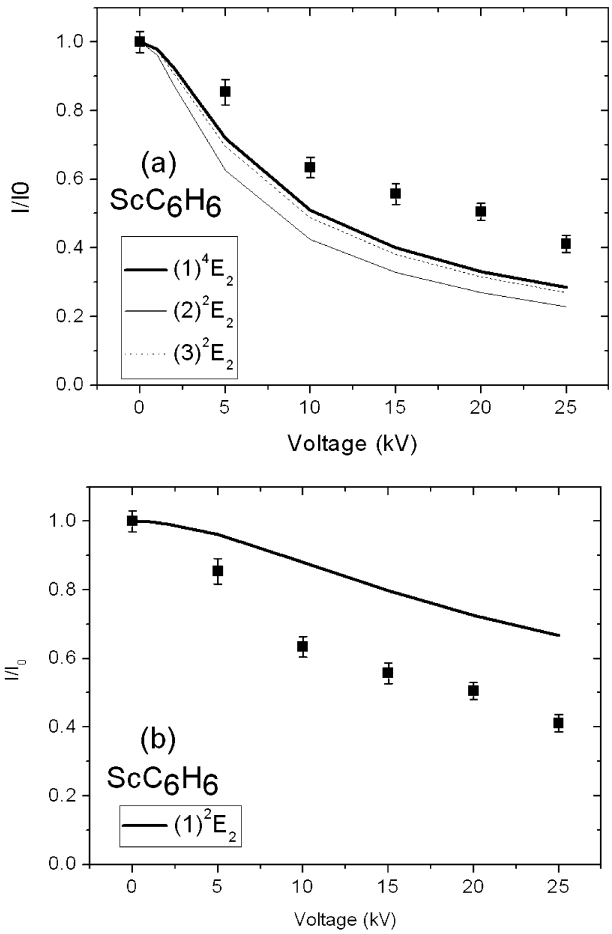

Figure 6. Relative intensity at the maximum of the ScC_6H_6 peak as a function of the voltage across the deflector. (a) Experimental results (■) and simulations for short-range states: (1) $^4E_2$ state ($\mu = 2.27$ D), (2) $^2E_2$ state ($\mu = 3.15$ D), and (3) $^2E_2$ state ($\mu = 2.44$ D). (b) Experimental results (■) and simulation for long-range states: (1) $^2E_2$ state ($\mu = 0.9$ D).

because there is almost no orientation of the molecules in the electric field. Results are shown in Figures 5−7. For clarity, we have separated the calculated curves for short- and long-distance states. For each complex, we have also fitted the value of the dipole on the experimental curves using the rotational constants corresponding to the lowest energy minimum. Results are given in Table 3.

VC_6H_6 Molecule. For the vanadium complex, the lowest electronic state $^4E_2$ has two minima: one at short distance and one at long distance. The electric dipole values of these two minima are very different. The dipole calculated for the short-distance-state minimum leads to a much stronger broadening than the experimental results (see the top panel of Figure 5). If we fitted the value of the dipole on the experimental results using the rotational constant of the quartet state at short distance, we would obtain a value of 0.12 D to be compared to the calculated value 2.79 D. This short-range minimum can be excluded. Experimental data are consistent with the simulation corresponding to the long-range minimum of the $^4E_2$ state. In this case, the experimental results suggest that we observe a long-range state. This state has the same multiplicity as the ground state of the vanadium atom (quartet). For this state, the fit of the experimental curve leads to a value of 0.17 ± 0.3 D that is slightly below the calculated dipole (0.6 D). We have no definitive explanation for this discrepancy. The agreement with the dipole calculated for the sextet state is poorer.

ScC_6H_6 Molecule. For the scandium complex, the minimum at short distance is a quartet while the minimum at long distance is a doublet ((1) $^2E_2$). This state has no pronounced minimum at short distance. Experimental results are compared to calculations in Figure 6. The situation is less clear than for vanadium. Experimental results are between what is expected for long-range and short-range states. We cannot draw a conclusion, and a mixing of long-range state and short-range state cannot be excluded with the present experimental results. The short-range quartet state might be observed because the relaxation toward the long-range state would imply a change of spin. This is

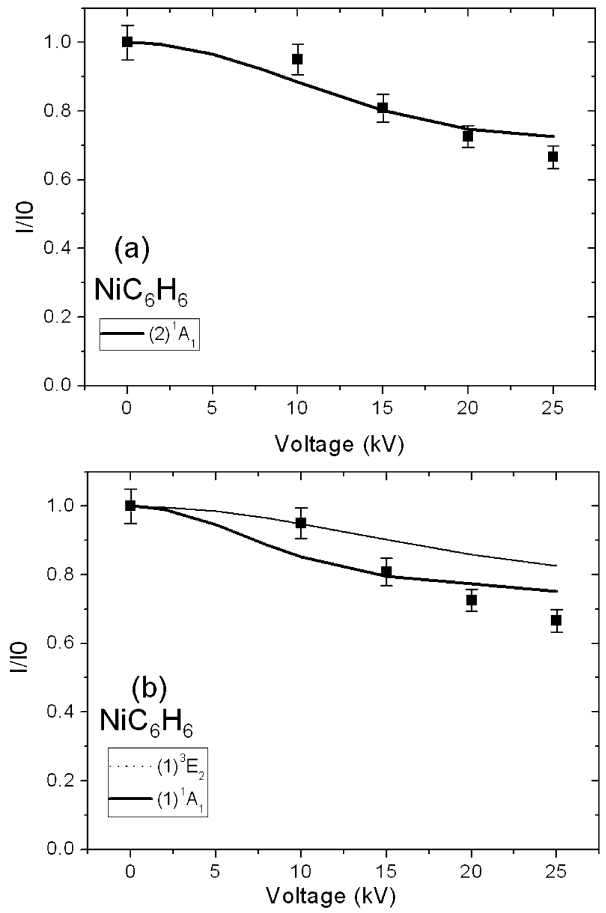

Figure 7. Relative intensity at the maximum of the NiC_6H_6 peak as a function of the voltage across the deflector. (a) Experimental results (■) and simulation for a short-range state: (2) $^1A_1$ state ($\mu = 0.49$ D). (b) Experimental results (■) and simulations for long-range states: (1) $^3E_2$ state ($\mu = 0.47$ D) and (1) $^1A_1$ state ($\mu = 0.9$ D).

TABLE 3: Experimental Dipole Moment μ (D) of MC_6H_6 Obtained Using the Rotational Constant Corresponding to the Lowest Energy Structure (Long-Range State)

molecule	dipole (D)	molecule	dipole (D)
ScC_6H_6	1.6 ± 0.3	NbC_6H_6	5.2 ± 0.5^a
VC_6H_6	0.17 ± 0.3	TaC_6H_6	0.7 ± 0.3^a
NiC_6H_6	0.7 ± 0.3		

[a] Dipole moment value derived using the rotational constant corresponding to the structure calculated for VC_6H_6 ((1) $^4E_2$ long-range state). For NbC_6H_6, the value obtained using the rotational constant corresponding to theVC_6H_6 (1) $^4E_2$ short-range geometry is 3.0 ± 0.3 D.

different from vanadium (see Figures 2 and 3). However, the formation of the short-range complex in the beam would imply the existence of metal atoms in long-lived excited states in the source. The excited ^4F state of the scandium atom lies 1.43 eV above the ^2D ground state. This state is not thermally populated but could be produced in the plasma during the laser vaporization process.

NiC_6H_6 Molecule. For the nickel complex, the ground (long-distance) state is a triplet while the most stable state at short distance is a singlet. These two minima have a similar dipole, but they do not have the same rotational constants, and a slightly different effect of the electric field is expected. The agreement for short-distance and long-distance states is similar and we cannot draw a conclusion. The atomic structure of the nickel atom is complex with a high density of levels near the ground state, corresponding to a competition between $3d^84s^2$ and

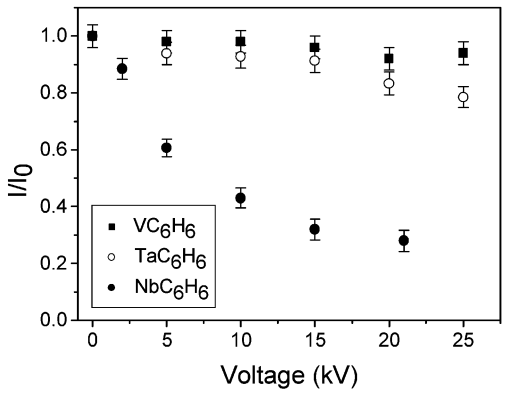

Figure 8. Experimental relative intensity at the maximum of the MC_6H_6 peak as a function of the voltage across the deflector (M =V, Nb, Ta). The decrease in intensity is a measurement of the broadening of the beam profile due to the electric field in the deflector.

$3d^94s^1$ configurations. As for scandium, there might be a coexistence of short- and long-range states. There may also be a coexistence of several long-range states.

NbC_6H_6 and TaC_6H_6 Molecules. Figure 8 shows the evolution of the relative intensity at the maximum of the peak as a function of the electric field for vanadium, tantalum, and niobium complexes. For niobium, a strong decrease is measured. On the other hand, a weak effect is observed for tantalum as for vanadium. These three metals are in the same column. The valence electron configuration is d^3s^2 for V and Ta, while it is d^4s^1 for Nb. Calculations have not been performed for Ta and Nb, but we used the equilibrium distance calculated for V (long-range state) to determine rotational constants and an experimental dipole from the curves plotted in Figure 8. The values are given in Table 3. Even if it is difficult to go further in the interpretation without calculations for Ta and Nb, the strong difference in the dipole values between Nb and V and Ta might be a signature of the difference in electronic structure and spin multiplicity of the metal−benzene complexes. It is interesting to note that, for vanadium, a higher dipole is calculated for the $^6A_1$ state (that is, correlated to the d^4s^1 metal atom excited state) than for the $^4E_2$ state (that is, correlated to the d^3s^2 ground state). The existence of a long-range state for NbC_6H_6 with an electric dipole of 5.2 D is unlikely. The observed large dipole may be the signature of a short-range state, as recently measured[9] for the TiC_6H_6 complex where the most stable short-range state is theoretically predicted to be stable against dissociation.[28]

Summary. CASSCF + MRCI calculations show that, for ScC_6H_6, VC_6H_6, and NiC_6H_6, there is no stable state at short metal−benzene distances. All the short-range-bound states are metastable with respect to the metal atom and benzene ground states. This was already noted in the case of vanadium complexes by Kaya and co-workers.[28] The only states below the dissociative limits are long-range states. It is difficult to estimate the lifetime of the metastable states, but as illustrated by Figures 2 and 3, there is a high density of states, and relaxation might be possible. In the case of vanadium, at the accuracy level of the present calculations, electric dipole measurements can only be interpreted with the existence of a long-range state. For Sc and Ni, results are also compatible with long-range states, but it is more difficult to draw a conclusion, and a mixing of long-range and short-range states in the beam cannot be excluded from these experiments. The electric dipoles deduced from the experiment using the long-range geometry are summarized in Table 3. The values obtained using short distances would be smaller but of the same order of magnitude (typically 1/3 lower). A particularity of long-range states is that

TABLE 4: Experimental Ionization Potential for Metal Atoms and Metal−Benzene Complexes[a]

molecule	IP(M)[b]	IP(MBz)[c]	$D_0(MBz^+)$[d]	$D_0(MBz)$[e]	$D_0(MBz)$[f] calcd	$D_0(MBz)$[g] calcd
ScC_6H_6	6.56	5.07	2.12	0.63	0.022	−1.03
VC_6H_6	6.75	5.11	2.42	0.78	0.030	−1.23
NiC_6H_6	7.64	5.99−6.42	2.52	0.87−1.3	0.031	−0.75

[a] Experimental and calculated dissociation energies for metal−benzene complexes. All the energies are given in electronvolts. [b] Ionization energy of the metal atom from ref 31. [c] Experimental ionization energy of the metal−benzene complex from ref 4. [d] Experimental dissociation energy of the complex cations from refs 7 and 29. [e] Dissociative energy of the metal−benzene complex deduced from the three precedent columns using $D_0(MBz) = D_0(MBz^+) + IP(MBz) - IP(M)$. [f] Calculated dissociative energy for the lowest energy state (long-range state). Relative energy with respect to the isolated benzene and the ground state of the metal atom. [g] Calculated dissociative energy for the lowest energy short-range state. Relative energy with respect to the isolated benzene and the ground state of the metal atom.

the potential energy curve is very flat. Changes in the distance between the benzene and the metal atom and corrections to the electric dipoles due to the external field were not taken into account.

6. Comparison with Estimated Dissociation Energies

Dissociative energies of the complexes ($MBz \rightarrow M + Bz$) can be estimated from experimental ionization potentials[4] and dissociative energies of the cations[7,29] using the formula $D_0(MBz) = D_0(MBz^+) + IP(MBz) - IP(M)$. The energies obtained with this formula are given in Table 4, with calculated values for short-range and long-range states. All the deduced values are positive and not consistent with the values calculated for short-range states, which are negative. For long-range states, calculated values are small but positive. The above formula should be used cautiously, because it is valid for an adiabatic value of IP(MBz). The experimental IP(MBz) is expected to be slightly higher than the adiabatic one. This may be particularly true for long-range states where the internuclear distances of MBz are very different from that of the MBz^+ ground state.[11,29] An overestimation of IP(MBz) would decrease the value of $D_0(MBz)$ and improve the agreement with the calculated values in Table 4.

In conclusion, the above energetic considerations are in favor of states that are stable against dissociation. At the present level of theory, the stable states for Sc, V, and Ni complexes correspond to long-range states. It should be noted that, for these systems, DFT calculations predict stable short-range states with a fragmentation energy in reasonable agreement with the values deduced from the dissiociation energies of the cation and the ionization potentials (see Table 4).[11,30] However, such single-reference-based calculations are known to favor states with the highest spin multiplicity and are expected to be less reliable for the characterization of the spin multiplicity than the CASSCF method. As a matter of fact, we have performed a DFT/B3LYP calculation for the VC_6H_6 complex. The ground state was found to be a sextet, while this state is found to be not stable in the present CASSCF study. The corresponding calculated dipole moment was found to be 3.58 D, while the experimental value (fitted using the corresponding rotational constant) is 0.12 D. The CASSCF + MRCI value of 0.6 D for the long-range $^4E_2$ ground state is in much better agreement with the experiment, though the CASSCF + MRCI method fails to reproduce the estimated dissociation energy.

7. Conclusion

In this paper we have reported electric beam deflection experiments for a series of isolated transition-metal−benzene complexes. Experimental results are compared to CASSCF + MRCI calculations. For every complex theoretically studied, the lowest energy structure was found, in the present work, to be a long-range state. These states have been determined for the first time. At least for the VC_6H_6 complex, the electric dipole measurement is clearly in favor of the existence of such a long-range state. In this paper we emphasize that these long-range states may play a critical role in the formation of metal−benzene complexes and cannot be ignored. The interaction between the benzene ring and transition metals remains difficult to compute. In particular, the discrepancy between DFT and CASSCF methods needs to be understood. A complete description of these systems is a challenge for both theoreticians and experimentalists.

References and Notes

(1) Muetterties, E. L.; Bleeke, J. R.; Wucherer, E. J.; Albright, T. A. *Chem. Rev.* **1982**, *82*, 499.

(2) Burdett, J. K.; Canadell, E. *Organometallics* **1985**, *4*, 805.

(3) Nakajima, A.; Kaya, K. *J. Phys. Chem. A* **2000**, *104*, 176.

(4) Kurikawa, T.; Takeda, H.; Hirano, M.; Judai, K.; Arita, T.; Nagao, S.; Nakajima, A.; Kaya, K. *Organometallics* **1999**, *18*, 1430.

(5) Weis, P.; Kemper, P. R.; Bowers, M. T. *J. Phys. Chem. A* **1997**, *101*, 8207.

(6) van Heijnsbergen, D.; von Helden, G.; Meijer, G.; Maitre, P.; Duncan, M. A. *J. Am. Chem. Soc.* **2001**, *124*, 1562.

(7) Meyer, F.; Khan, F. A.; Armentrout, P. B. *J. Am. Chem. Soc.* **1995**, *117*, 9740.

(8) Imura, K.; Kawashima, T.; Ohoyama, H.; Kasai, T. *J. Am. Chem. Soc.* **2001**, *123*, 6367.

(9) Imura, K.; Ohoyama, H.; Kasai, T. *Chem. Phys. Lett.* **2003**, *369*, 55.

(10) Rayane, D.; Allouche, A. R.; Antoine, R.; Broyer, M.; Compagnon, I.; Dugourd, P. *Chem. Phys. Lett.* **2003**, *375*, 506.

(11) Pandey, R.; Rao, B. K.; Jena, P.; Blanco, M. A. *J. Am. Chem. Soc.* **2001**, *123*, 3799.

(12) Froudakis, G. E.; Andriotis, A. N.; Menon, M. *Chem. Phys. Lett.* **2001**, *350*, 393.

(13) Yang, C.-N.; Klippenstein, S. J. *J. Phys. Chem. A* **1999**, *103*, 1094.

(14) Rao, B. K.; Jena, P. *J. Chem. Phys.* **2002**, *116*, 1343.

(15) Yasuike, T.; Yabushita, S. *J. Phys. Chem. A* **1999**, *103*, 4533.

(16) Cloke, F. G. N.; Dix, A. N.; Green, J. C.; Perutz, R. N.; Seddon, E. A. *Organometallics* **1983**, *2*, 1150.

(17) Andrews, M. P.; Mattar, S. M.; Ozin, G. A. *J. Phys. Chem.* **1986**, *90*, 1037.

(18) Andrews, M. P.; Mattar, S. M.; Ozin, G. A. *J. Phys. Chem.* **1986**, *90*, 744.

(19) Dugourd, P.; Compagnon, I.; Lepine, F.; Antoine, R.; Rayane, D.; Broyer, M. *Chem. Phys. Lett.* **2001**, *336*, 511.

(20) Ekstrom, C. R.; Schmiedmayer, J.; Chapman, M. S.; Hammond, T. D.; Pritchard, D. E. *Phys. Rev. A* **1995**, *51*, 3883.

(21) MOLPRO is a package of ab initio programs written by H. J. Werner and P. J. Knowles, with contibutions from R. D. Amos, A. Berning, D. L. Cooper, et al., University of Birmingham, 2000.

(22) Dolg, M.; Wedig, U.; Stoll, H.; Preuss, H. *J. Chem. Phys.* **1987**, *86*, 866.

(23) Igel-Mann, J.; Stoll, H.; Preuss, H. *Mol. Phys.* **1988**, *65*, 1321.

(24) Stevens, W. J.; Basch, H.; Krauss, M. *J. Chem. Phys.* **1984**, *81*, 6026.

(25) Stevens, W. J.; Krauss, M.; Basch, H.; Jasien, P. G. *Can. J. Chem.* **1992**, *70*, 612.

(26) Hong, G.; Schautz, F. *J. Am. Chem. Soc.* **1999**, *121*, 1502.

(27) Sugar, J.; Corliss, C. *J. Phys. Chem. Ref. Data* **1985**, *14*, 1.

(28) Yasuike, T.; Nakajima, A.; Yabushita, S.; Kaya, K. *J. Phys. Chem. A* **1997**, *101*, 5360.

(29) Bauschlicher, C. W.; Partridge, H.; Langhoff, S. R. *J. Phys. Chem.* **1992**, *96*, 3273.

(30) Chaquin, P.; Costa, D.; Lepetit, C.; Che, M. *J. Phys. Chem. A* **2001**, *105*, 4541.

(31) Lide, D. R. *CRC Handbook of Chemistry and Physics*; CRC Press: Boca Raton, FL, 1999.